

Avalanche Dynamics for Active Matter in Heterogeneous Media

C. J. O. Reichhardt and C. Reichhardt

Theoretical Division and Center for Nonlinear Studies, Los Alamos National Laboratory, Los Alamos, New Mexico 87545, USA

E-mail: cjrx@lanl.gov

Abstract. Using numerical simulations, we examine the dynamics of active matter run-and-tumble disks moving in a disordered array of obstacles. As a function of increasing active disk density and activity, we find a transition from a completely clogged state to a continuous flowing phase, and in the large activity limit, we observe an intermittent state where the motion occurs in avalanches that are power law distributed in size with an exponent of $\beta = 1.46$. In contrast, in the thermal or low activity limit we find bursts of motion that are not broadly distributed in size. We argue that in the highly active regime, the system reaches a self-jamming state due to the activity-induced self-clustering, and that the intermittent dynamics is similar to that found in the yielding of amorphous solids. Our results show that activity is another route by which particulate systems can be tuned to a nonequilibrium critical state.

1. Introduction

There are numerous examples of driven collectively interacting systems that exhibit avalanches or intermittent behavior when driven over quenched disorder, including vortices in type-II superconductors [1, 2, 3], magnetic domain walls [4, 5], earthquake models [6, 7], and colloidal depinning over rough landscapes [8]. At a critical driving force F_c , there is a depinning transition from a pinned to a sliding state. Motion often occurs in avalanches close to the depinning transition, and if depinning is associated with critical features such as diverging characteristic lengths and times, the avalanches and other fluctuating quantities will exhibit broad or power law distributions [5, 7]. Scale-free avalanche dynamics often appear near yielding or unjamming transitions, such as in the intermittent motion of dislocations in crystalline solids [9, 10, 11] or the rearrangements of particles at yielding in amorphous materials [12, 13, 14, 15]. For loose assemblies of particles such as grains or bubbles, the shear modulus becomes finite above a density ϕ_j when a jamming transition occurs [16, 17], and it is known that in such systems, the dynamics become increasingly intermittent as the jamming point is approached, producing power law distributions in a variety of dynamic quantities [18, 19, 20, 21, 22, 23].

In the driven systems described above, the dynamics arise from some form of externally applied driving or shear. In contrast, in active matter systems the particles are *self*-driven. Examples of active matter systems that have been attracting increasing attention include pedestrian flow, biological systems such as run-and-tumble bacteria, and self-propelled colloids [24, 25]. The behavior of these systems can be captured by a simple model consisting of sterically interacting hard disks with a self-mobility represented either by driven diffusion or run-and-tumble dynamics. In two dimensions, a non-active, thermal assembly of hard disks forms a uniform density liquid at finite temperature, and if the disk density is large enough, a jammed or crystalline state emerges [17]. If the disks are self-propelled or active, for large enough activity a transition can occur from the uniform liquid state to a phase separated state in which a high density cluster that can be regarded as a solid is surrounded by a low density gas of disks, even when the overall density of the system is well below that at which non-active disks would jam or crystallize [26, 27, 28]. Self-clustering occurs when multiple active disks collide and continue to swim into each other, producing an active load-bearing contact in a system containing no tensile forces, and it has been observed in experiments using self-propelled colloids [29, 30] and in simulations of disks obeying driven diffusive or run-and-tumble dynamics [28]. Previous numerical studies [31] of active run-and-tumble disks driven through random obstacle arrays show that for fixed active disk density, the average drift mobility of the disks is a nonmonotonic function of the activity, initially increasing with increasing run length, but then passing through a maximum and decreasing at large run lengths, with the onset of self-clustering or self-jamming coinciding with the mobility reduction. For a fixed run length, the mobility decreases as the active disk density increases due to crowding effects.

In this work we examine the motion of active run-and-tumble disks driven through a random obstacle array as a function of obstacle density and activity. We find that there is a critical amount of disorder and activity above which the motion becomes highly intermittent and takes the form of avalanches that are power law distributed in size, $P(s) \propto s^{-\beta}$, with an exponent of $\beta = 1.46 \pm 0.1$. For fixed obstacle density but decreasing activity, the motion becomes more continuous, the avalanche behavior is lost, and the disks act like a fluid moving through the obstacle array, while at zero or

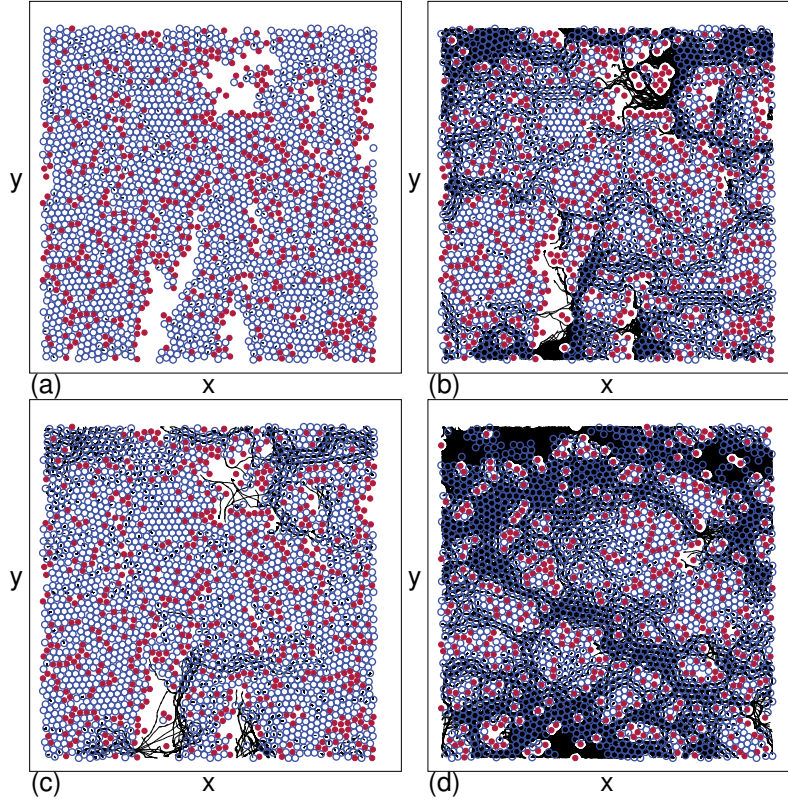


Figure 1. The obstacle positions (red filled circles), active disks (dark blue open circles), and trajectories (light blue lines) for a system with $\phi_{\text{tot}} = 0.754$. (a) For low activity $l_r = 0.1$ at $\phi_{\text{obs}} = 0.1727$, the disks become completely clogged and there is no motion. (b) For intermediate activity $l_r = 1$ at $\phi_{\text{obs}} = 0.1727$, we find a combination of flowing and immobile active disks. (c) For high activity $l_r = 320$ at $\phi_{\text{obs}} = 0.1727$, motion occurs only in bursts or avalanches. (d) A system with $l_r = 320$ at a lower obstacle density of $\phi_{\text{obs}} = 0.1256$.

very small activity, the disks become completely clogged and there is no motion. We argue that in the limit of large activity, critical behavior occurs due to self-jamming or self-clustering, while in the low but finite activity limit the disks act like a liquid with continuous fluctuations. The critical behavior under an external drive can be viewed as analogous to a yielding transition of an amorphous solid close to a jamming point. We also find that for fixed active disk density, a critical amount of disorder in the form of obstacles must be added to produce power law distributed avalanche sizes, similar to the behavior observed for avalanches in certain magnetic systems [5, 32, 33]. Our results indicate that activity can provide another method for tuning a system to a nonequilibrium critical state.

2. Simulation

We simulate a two-dimensional $L \times L$ system with $L = 50$ and with periodic boundary conditions in the x and y -directions containing N_{obs} obstacles and N_a active disks of radius $R = 0.5$. The obstacles are identical to the active disks except their

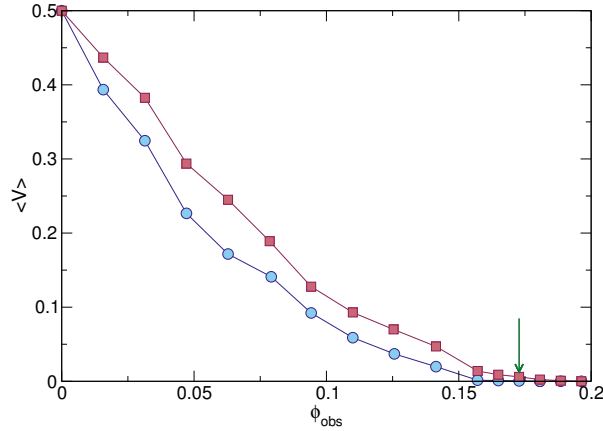


Figure 2. Average active disk velocity $\langle V \rangle$ in the direction of the applied drive vs ϕ_{obs} for a system with $\phi_{\text{tot}} = 0.754$ at $l_r = 1$ (red squares) and $l_r = 320$ (blue circles). The green arrow indicates the value of ϕ_{obs} used in Fig. 3.

locations are permanently fixed. Steric disk-disk interactions are given by a harmonic repulsive force $\mathbf{F}_{dd} = k(d - 2R)\Theta(d - 2R)\hat{\mathbf{d}}$ where d is the distance and $\hat{\mathbf{d}}$ is the displacement vector between a pair of disks. The spring constant $k = 100$ is large enough that, for the parameters we consider, disks overlap by less than $0.01R$, so the system is approximately in the hard disk limit. The obstacle area coverage is $\phi_{\text{obs}} = N_{\text{obs}}\pi R^2/L^2$, the active disk area coverage is $\phi_a = N_a\pi R^2/L^2$, and the total area coverage is $\phi_{\text{tot}} = \phi_{\text{obs}} + \phi_a$. In an obstacle-free system with $\phi_{\text{obs}} = 0$, in the absence of activity the disks form a hexagonal solid near $\phi_a = 0.9$. The active disk dynamics obey the following overdamped equation of motion:

$$\eta \frac{d\mathbf{r}_i}{dt} = \mathbf{F}_{\text{inter}}^i + \mathbf{F}_m^i + \mathbf{F}_{\text{obs}}^i + \mathbf{F}_D \quad (1)$$

where the damping coefficient $\eta = 1$. The interactions between active disks are given by $\mathbf{F}_{\text{inter}}^i = \sum_j^{N_a} \mathbf{F}_{dd}^{ij}$, and $\mathbf{F}_m^i = F_m \hat{\mathbf{m}}^i$ is a run-and-tumble motor force with $F_m = 0.5$ that acts in a randomly chosen running direction $\hat{\mathbf{m}}^i$ for a running time τ , after which a new running direction $\hat{\mathbf{m}}^{i'}$ is randomly chosen. In the absence of any collisions, during the running time an active disk moves a run length $l_r = F_m \tau \delta t$, where $\delta t = 0.002$ is the simulation time step. The obstacle forces are given by $\mathbf{F}_{\text{obs}}^i = \sum_k^{N_{\text{obs}}} \mathbf{F}_{dd}^{ik}$, and the external driving force $\mathbf{F}_D = F_D \hat{\mathbf{x}}$ is applied uniformly to all active disks with $F_D = 0.5$. To initialize the system, we place a density ϕ_{tot} of disks at nonoverlapping locations in the sample, and then randomly choose N_{obs} of the disks to serve as obstacles, fixing them in their original random locations. We apply a driving force \mathbf{F}_D and wait several million simulation time steps to ensure that we have reached a steady state before measuring the active disk velocity fluctuations and displacements. We obtain a time series of the average active disk velocity in the driving direction, $V(t) = N_a^{-1} \sum_i^{N_a} v_i^x(t)$, where $v_i^x(t) = \mathbf{v}_i(t) \cdot \hat{\mathbf{x}}$, and also measure the time-averaged active disk velocity in the driving direction $\langle V \rangle = \langle V(t) \rangle$. We quantify the activity level using l_r and the disorder using ϕ_{obs} .

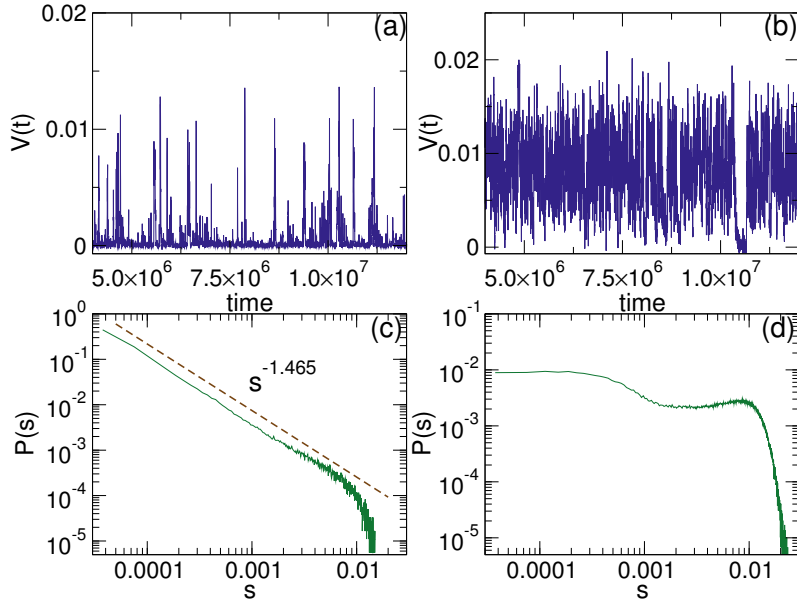


Figure 3. (a) A portion of the time series of the average disk velocity $V(t)$ from the system in Fig. 2 at $\phi_{\text{tot}} = 0.754$, $\phi_{\text{obs}} = 0.1727$, and $l_r = 320$, where the motion is strongly intermittent. (b) The avalanche size distribution $P(s)$ from the complete time series for the system in panel (a). The dashed line is a power law fit with exponent $\beta = 1.465 \pm 0.15$. (c) $V(t)$ for the $l_r = 1$ system from Fig. 2. (d) $P(s)$ for the system in panel (c) has a bimodal rather than a power law shape.

3. Results

In Fig. 1 we illustrate the behavior of a system with $\phi_{\text{tot}} = 0.754$. For $\phi_{\text{obs}} = 0.1727$, Fig. 1(a) shows that at a very low activity level of $l_r = 0.1$, the disks become completely clogged with $\langle V \rangle = 0$. In Fig. 1(b) at a higher level of activity $l_r = 1$, we find a coexistence of jammed and moving active disks, while for large activity $l_r = 320$ in Fig. 1(c), the flow is highly intermittent and occurs through avalanches. Figure 1(d) shows that in an $l_r = 320$ system with a lower obstacle density of $\phi_{\text{obs}} = 0.1256$, the flow of active disks becomes continuous again.

In Fig. 2 we plot the average drift velocity per active disk in the direction of drive $\langle V \rangle$ versus ϕ_{obs} over the range $0 \leq \phi_{\text{obs}} \leq 0.196$ for a system with $\phi_{\text{tot}} = 0.754$ at $l_r = 1$ and $l_r = 320$. As shown in previous work [34], self clustering occurs when $l_r > 10$ for $\phi_{\text{tot}} = 0.754$, so the values of l_r in Fig. 2 are representative of the liquid state and the phase separated state. At $\phi_{\text{obs}} = 0$ the disks undergo free flow drift giving $\langle V \rangle = F_D = 0.5$ for all l_r ; however, as ϕ_{obs} increases, $\langle V \rangle$ is always lower in the phase separated $l_r = 320$ sample than in the liquid $l_r = 1$ sample. For $\phi_{\text{obs}} > 0.15$, the motion in the $l_r = 320$ system becomes highly intermittent, as shown by the plot of $V(t)$ in Fig. 3(a) for the system in Fig. 2 with $l_r = 320$ at $\phi_{\text{obs}} = 0.1727$, which is also illustrated in Fig. 1(c). Here the motion occurs in bursts or avalanches. In contrast, the $l_r = 1$ sample at the same obstacle density has a much more continuous $V(t)$, as shown in Fig. 3(b) and illustrated in Fig. 1(b). The average velocity ratio $\langle V \rangle_{l_r=1} / \langle V \rangle_{l_r=360} = 17$ for $\phi_{\text{obs}} = 0.1727$, indicating how strongly an increase in activity can reduce the flow through the system. We use the time series $V(t)$ to

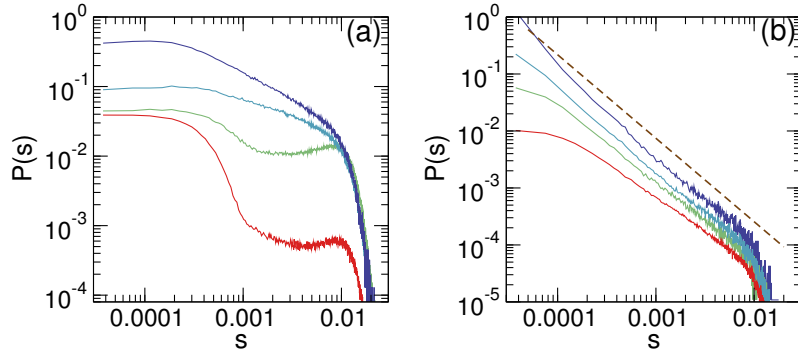


Figure 4. Avalanche size distribution $P(s)$ for a system with $\phi_{\text{tot}} = 0.754$ and $\phi_{\text{obs}} = 0.1727$. (a) $l_r = 0.3$ (red), 1.0 (green), 10 (light blue), and 20 (dark blue), from bottom to top. The curves have been shifted vertically for clarity. (b) $l_r = 80$ (red), 160 (green), 320 (light blue), and 640 (dark blue), from bottom to top. The curves have been shifted vertically for clarity. The dashed line indicates a power law fit with exponent $\beta = 1.465$.

construct an avalanche size distribution $P(s)$, where s is defined to be equal to the instantaneous value of V . In Fig. 3(b), $P(s)$ for the $l_r = 320$ system can be fit to a power law distribution over two decades with an exponent $\beta = 1.465 \pm 0.15$, while in Fig. 3(d), $P(s)$ for the $l_r = 1$ system is not broad but has a bimodal distribution, where the second peak is characteristic of the flow of a liquid through a disordered medium [8].

In Fig. 4(a) we plot $P(s)$ for a system with $\phi_{\text{tot}} = 0.754$ and $\phi_{\text{obs}} = 0.1727$ at $l_r = 0.3, 1.0, 10,$ and 20 . The bimodal characteristics of the $l_r = 0.3$ and $l_r = 1.0$ distributions are lost for $l_r = 10$ when the system acts like a fluid. The avalanche size distribution broadens when self-induced clustering begins to occur, and for $l_r = 20$ and above it is possible to fit a power law to a portion of $P(s)$. Fig. 4(b) shows $P(s)$ for the same system at $l_r = 80, 160, 320,$ and 640 along with a dashed line indicating a power law fit with exponent $\beta = 1.465$. The region over which $P(s)$ obeys a power law grows in extent as l_r increases, and the exponent falls in the range $1.35 \leq \beta \leq 1.5$. The overall shape of $P(s)$ remains nearly the same for $l_r = 80$ and above, but the time intervals separating successive avalanche events increase with increasing l_r . These results indicate that there is a critical r_l above which scale-free avalanches occur, and that this critical value corresponds to the point at which the system begins to act like a solid rather than a liquid.

In Fig. 5(a) we plot $\langle V \rangle$ versus l_r for the system in Fig. 2 at $\phi_{\text{tot}} = 0.754$ and $\phi_{\text{obs}} = 0.1727$. Based on the behavior of the $P(s)$ distributions, as illustrated in Fig. 4, we identify three regimes: a fully clogged state for $l_r \leq 0.2$, where $\langle V \rangle = 0$ as illustrated in Fig. 1(a), a flowing or liquidlike region for $0.2 < l_r < 20$, and an intermittent avalanche regime for $l_r \geq 20$. We measure the fraction c of disks that belong to the largest cluster using the cluster identification algorithm described in [35], and in Fig. 5(b) we plot c versus l_r for an obstacle-free sample with the same $\phi_{\text{tot}} = 0.754$ as in Fig. 5(a) but with $\phi_{\text{obs}} = 0$, showing that the onset of the intermittent phase in the presence of obstacles correlates with a large increase in self-clustering in the absence of obstacles.

The avalanche size distributions are also affected by the obstacle density. In

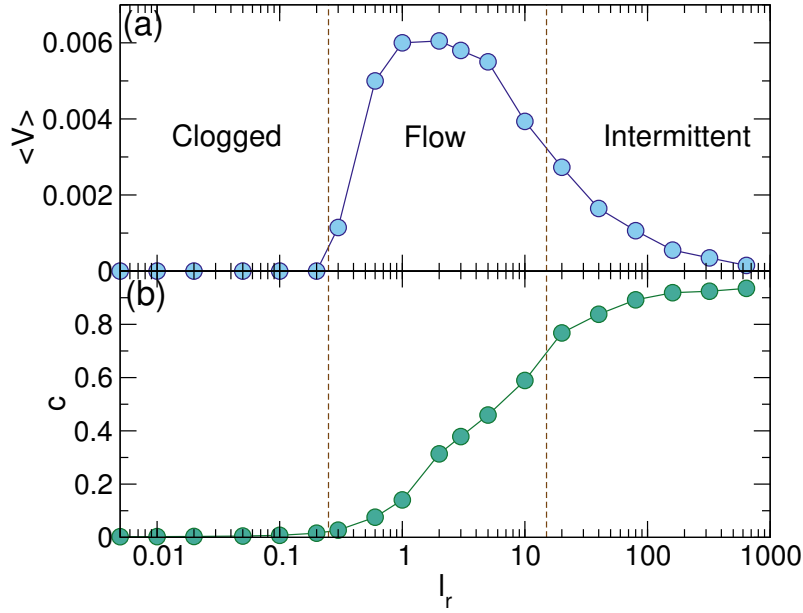


Figure 5. The time-average disk flux through the system $\langle V \rangle$ vs l_r for samples with $\phi_{\text{tot}} = 0.754$ and $\phi_{\text{obs}} = 0.1727$ showing the completely clogged regime at low l_r , the flow regime at intermediate l_r , and the intermittent or avalanche regime at large l_r . (b) The fraction c of disks that are in the largest cluster vs l_r for a system with $\phi_{\text{tot}} = 0.754$ and $\phi_{\text{obs}} = 0$, showing that the onset of the intermittent phase correlates with the onset of self-clustering.

Fig. 6(a) we plot $P(s)$ for fixed $\phi_{\text{tot}} = 0.754$ and $l_r = 320$ at $\phi_{\text{obs}} = 0.1413, 0.157$, and 0.1727 . For $\phi_{\text{obs}} = 0.1413$, even though the system can self-cluster there is enough room for the disk clusters to flow freely around the obstacles, giving a peak at a characteristic avalanche size $s \approx 0.03$, while at $\phi_{\text{obs}} = 0.157$, avalanches of size $s > 0.2$ are lost and $P(s)$ begins to broaden. In Fig. 6(b) we plot $P(s)$ for the same system with $\phi_{\text{obs}} = 0.1727, 0.1884$, and 0.2 . The maximum avalanche size s_{max} continues to decrease as the obstacle density increases, and at $\phi_{\text{obs}} = 0.2041$ the avalanche motion is completely suppressed since $\langle V \rangle = 0$. This behavior is similar to what has been predicted for models of avalanches in magnetic systems, where it is necessary to add a critical amount of disorder in order to obtain avalanches that are power law distributed in size [5, 32, 33]. For weak disorder the magnetic avalanches are dominated by system spanning events, while for strong disorder only small avalanches occur.

In Fig. 7 we show $P(s)$ for a system with fixed $\phi_{\text{obs}} = 0.1727$ and $l_r = 320$ at $\phi_{\text{tot}} = 0.377, 0.5, 0.628$, and 0.754 , along with a power law fit with exponent $\beta = 1.465$. For $\phi_{\text{tot}} = 0.377$ and $\phi_{\text{tot}} = 0.5$, $P(s)$ cannot be fit by a single power law, while for $\phi_{\text{tot}} = 0.65$ and $\phi_{\text{tot}} = 0.754$, there is good agreement with the power law fit, indicating that critical behavior only appears when the system is not too sparse.

4. Discussion

We ask where the criticality we observe in our active matter system originates. When l_r and ϕ_a are large enough, the obstacle-free system enters a phase separated state

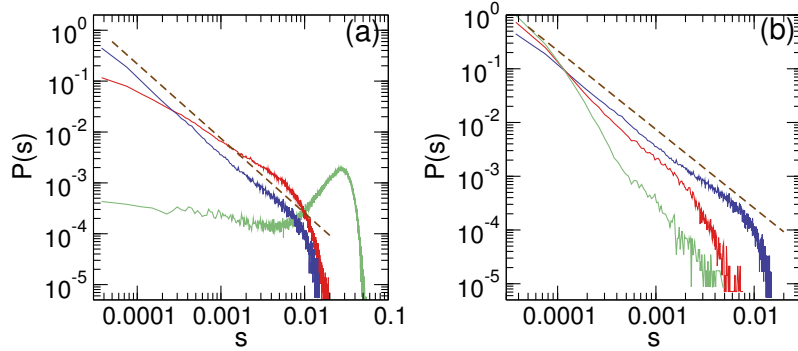


Figure 6. Avalanche size distributions $P(s)$ for a system with $\phi_{\text{tot}} = 0.754$ and $l_r = 320$ at (a) $\phi_{\text{obs}} = 0.1413$ (green), 0.157 (red) and 0.1727 (blue). (b) The same for $\phi_{\text{obs}} = 0.1727$ (blue), 0.1884 (red), and 0.2 (green). The dashed lines are power law fits with $\beta = 1.465$.

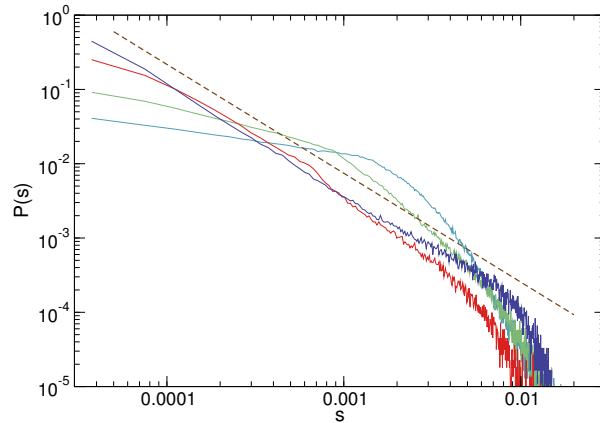


Figure 7. $P(s)$ for a system with $\phi_{\text{obs}} = 0.1727$ and $l_r = 320$ at $\phi_{\text{tot}} = 0.377$ (light blue), 0.5 (green), 0.628 (red), and 0.754 (dark blue). The dashed line is a power law fit with exponent $\beta = 1.465$.

in which the dense cluster regions have a density close to the jamming density, so the dense regions can be viewed as an assembly of grains that is close to the critical Point J identified in Ref. [16]. Several studies of yielding in two-dimensional foams [36] and granular matter [37] identify avalanches that have a power law size distribution with an exponent of $\beta = 1.5$, while other simulations of yielding in two-dimensional granular matter give avalanches with power law size distribution exponents of $\beta = 1.43$ [38]. The exponent we observe is close to the value $\beta = 1.5$ predicted using mean field models [39, 40]. There are also studies of yielding in soft particulate matter systems in which avalanches with exponents $\beta = 1.35$ appear [41], while experiments on frictional granular matter give avalanche exponents of $\beta = 1.24$ [38]. We argue that in the thermal limit of small l_r , our active disks behave like a liquid with short correlation lengths, so portions of the system can readily flow as long as there is space for motion between the obstacles. When $l_r = 0$ in the limit of zero activity, the disks reach a completely clogged state where no fluctuations and therefore no avalanches occur. At large l_r , the disks self-cluster and locally behave like a granular solid just

on the verge of jamming, where large correlation lengths emerge, but the fact that the disks are active and are always attempting to move prevents the system from becoming permanently trapped in a jammed state. Instead, occasional activity-induced unjamming events occur that have the appearance of avalanches. The motion of our active disks is impeded by the presence of obstacles; however, even in the absence of obstacles, the active clusters can undergo local rearrangements that can occur suddenly as an avalanche. In previous simulations of active disks without obstacles, local velocity fluctuations of a single driven probe disk were power law distributed with an exponent of $\beta = 2.0$ when the activity was large enough to permit self-clustering to occur, while in the low activity limit where the system acts like a uniform fluid, the velocity fluctuation distribution was exponential [34].

In this work we focus on the case where there is an applied drive in order to characterize the avalanche behavior; however, it would also be interesting to study a dense active disk assembly in the presence of quenched disorder rather than obstacles to see whether avalanches also occur in the absence of an external drift force. Previous numerical simulations of active disks on quenched disorder have only explored the low density regime [42]. It would also be interesting to determine whether other active matter models such as flocking particles exhibit avalanche behavior in the presence of quenched disorder. Simulations have already shown nonmonotonic transport behavior in such systems [43] as well as disorder-induced transitions from flocking to non-flocking states [44], and there are now experimental realizations of flocking systems with quenched disorder [45] that could be used to explore this issue.

5. Summary

We have numerically examined the avalanche behavior of active matter composed of run-and-tumble disks driven through a random obstacle array. We measure avalanche sizes in terms of the average instantaneous velocity of the active disks. At low activity the system becomes trapped in a completely clogged state, while at intermediate levels of activity the disks act like a fluid that can flow continuously among the obstacles, producing a bimodal avalanche size distribution. At large run lengths, the disks undergo self-clustering and their motion becomes highly intermittent, taking the form of avalanches of correlated disk motion that have a power law size distribution with an exponent of $\beta = 1.465$. We argue that the intermittency results from self-clustering, which causes the system to act like a granular solid that is near the jamming point, and that the activity-induced avalanches are similar to the behavior observed in the yielding of marginally stable solids such as foams or granular packings, where avalanches with similar size distribution power law exponents appear. Finally, we find that when the density of obstacles is large enough, the avalanche size distribution is cut off at large sizes, suggesting that there is a critical disorder density that maximizes the critical nature of the avalanches. Our results indicate that activity provides another route for creating critical nonequilibrium states in particulate matter.

Acknowledgments

This work was carried out under the auspices of the NNSA of the U.S. DoE at LANL under Contract No. DE-AC52-06NA25396.

References

- [1] Olson C J, Reichhardt C and Nori F 1997 Superconducting vortex avalanches, voltage bursts, and vortex plastic flow: Effect of the microscopic pinning landscape on the macroscopic properties *Phys. Rev. B* **56** 6175
- [2] Bassler K and Paczuski M 1998 Simple model of superconducting vortex avalanches *Phys. Rev. Lett.* **81** 3761
- [3] Altshuler E 2004 Experiments in vortex avalanches *Rev. Mod. Phys.* **76** 471
- [4] Zapperi S, Cizeau P, Durin G and Stanley H E 1998 Dynamics of a ferromagnetic domain wall: Avalanches, depinning transition, and the Barkhausen effect *Phys. Rev. B* **58** 6353
- [5] Sethna J P, Dahmen K and Myers C R 2001 Crackling noise *Nature* **410** 242
- [6] Carlson J M and Langer J S 1989 Properties of earthquakes generated by fault dynamics *Phys. Rev. Lett.* **62** 2632
- [7] Fisher D S 1998 Collective transport in random media: From superconductors to earthquakes *Phys. Rep.* **301** 113
- [8] Reichhardt C and Reichhardt C J O 2017 Depinning and nonequilibrium dynamic phases of particle assemblies driven over random and ordered substrates: A review *Rep. Prog. Phys.* **80** 026501
- [9] Miguel M-C, Vespignani A, Zapperi S, Weiss J and Grasso J-R 2001 Intermittent dislocation flow in viscoplastic deformation *Nature* **410** 667
- [10] Zaiser M 2006 Scale invariance in plastic flow of crystalline solids *Adv. Phys.* **55** 185
- [11] McDermott D, Reichhardt C J O and Reichhardt C 2016 Avalanches, plasticity, and ordering in colloidal crystals under compression *Phys. Rev. E* **93** 062607
- [12] Salerno K M, Maloney C E and Robbins M O 2012 Avalanches in strained amorphous solids: Does inertia destroy critical behavior? *Phys. Rev. Lett.* **109** 105703
- [13] Lin Jie, Gueudre T, Rosso A and Wyart M 2015 Criticality in the approach to failure in amorphous solids *Phys. Rev. Lett.* **115** 168001
- [14] Regev I, Weber J, Reichhardt C, Dahmen K A and Lookman T 2015 Reversibility and criticality in amorphous solids *Nature Commun.* **6** 8805
- [15] Nicolas A, Ferrero E E, Martens K and Barrat J-L 2017 Deformation and flow of amorphous solids: a review of mesoscale elastoplastic models *Preprint* arXiv:1708.09194
- [16] Liu A J and Nagel S R 1998 Nonlinear dynamics: Jamming is not just cool any more *Nature* **396** 21
- [17] Reichhardt C and Reichhardt C J O 2014 Aspects of jamming in two-dimensional athermal frictionless systems *Soft Matter* **10** 2932
- [18] Drocco J A, Hastings M B, Reichhardt C J O and Reichhardt C 2005 Multiscaling at point J: Jamming is a critical phenomenon *Phys. Rev. Lett.* **95** 088001
- [19] Candelier R and Dauchot O 2010 Journey of an intruder through the fluidization and jamming transitions of a dense granular media *Phys. Rev. E* **81** 011304
- [20] Reichhardt C J O and Reichhardt C 2010 Fluctuations, jamming, and yielding for a driven probe particle in disordered disk assemblies *Phys. Rev. E* **82** 051306
- [21] Arévalo R and Ciamarra M P 2014 Size and density avalanche scaling near jamming *Soft Matter* **10** 2728
- [22] Woldhuis E, Chikkadi V, van Deen M S, Schall P and van Hecke M 2015 Fluctuations in flows near jamming *Soft Matter* **11** 7024
- [23] Franz S and Spigler S 2017 Mean-field avalanches in jammed spheres *Phys. Rev. E* **95** 022139
- [24] Ramaswamy S 2010 The mechanics and statistics of active matter *Annu. Rev. Condens. Matter Phys.* **1** 323
- [25] Bechinger C, Di Leonardo R, Löwen H, Reichhardt C, Volpe G and Volpe G 2016 Active Brownian particles in complex and crowded environments *Rev. Mod. Phys.* **88** 045006
- [26] Fily Y and Marchetti M C 2012 Athermal phase separation of self-propelled particles with no alignment *Phys. Rev. Lett.* **108** 235702
- [27] Redner G S, Hagan M F and Baskaran A 2013 Structure and dynamics of a phase-separating active colloidal fluid *Phys. Rev. Lett.* **110** 055701
- [28] Cates M A and Tailleur J 2015 Motility-induced phase separation *Annu. Rev. Condens. Mat. Phys.* **6** 219
- [29] Palacci P, Sacanna S, Steinberg A P, Pine D J, and Chaikin P M 2013 Living crystals of light-activated colloidal surfers *Science* **339** 936
- [30] Buttinoni I, Bialké J, Kümmel F, Löwen H, Bechinger C and Speck T 2013 Dynamical clustering and phase separation in suspensions of self-propelled colloidal particles *Phys. Rev. Lett.* **110** 238301

- [31] Reichhardt C and Reichhardt C J O 2014 Active matter transport and jamming on disordered landscapes *Phys. Rev. E* **90** 012701
- [32] Perkovic O, Dahmen K and Sethna J P 1995 Avalanches, Barkhausen noise, and plain old criticality *Phys. Rev. Lett.* **75** 4528
- [33] Chern G-W, Reichhardt C and Reichhardt C J O 2014 Avalanches and disorder-induced criticality in artificial spin ices *New J. Phys.* **16** 063041
- [34] Reichhardt C and Reichhardt C J O 2015 Active microrheology in active matter systems: Mobility, intermittency, and avalanches *Phys. Rev. E* **91** 032313
- [35] Luding S and Herrmann H J 1999 Cluster growth in freely cooling granular media *Chaos* **9** 673
- [36] Kabla A, Scheibert J and Debregeas G 2007 Quasistatic rheology of foams: II. Transition to shear banding *J. Fluid Mech.* **587** 45
- [37] Hayman N W, Ducloue L, Foco K L and Daniels K E 2011 Granular controls on periodicity of stick-slip events: kinematics and force-chains in an experimental fault *Pure Appl. Geophys.* **168** 2239
- [38] Barés J, Wang D, Wang D, Bertrand T, O'Hern C S and Behringer R P 2017 Local and global avalanches in a 2D sheared granular medium *Preprint* arXiv:1709.01012
- [39] Dahmen K, Ben-Zion Y and Uhl J T 2009 Micromechanical model for deformation in solids with universal predictions for stress strain curves and slip avalanches *Phys. Rev. Lett.* **102** 175501
- [40] Salje E K H and Dahmen K A 2014 Crackling noise in disordered materials *Ann. Rev. Condens. Mat. Phys.* **5** 233
- [41] Lin J, Lerner E, Rosso A and Wyart M 2014 Scaling description of the yielding transition in soft amorphous solids at zero temperature *Proc. Natl. Acad. Sci. (USA)* **111** 14382
- [42] Zeitz M, Wolff K and Stark H 2017 Active Brownian particles moving in a random Lorentz gas *Eur. Phys. J.E* **40** 23
- [43] Chepizhko O, Altmann E G and Peruani F 2013 Optimal noise maximizes collective motion in heterogeneous media *Phys. Rev. Lett.* **110** 238101
- [44] Quint D and Gopinathan A 2015 Topologically induced swarming phase transition on a 2D percolated lattice *Phys. Biol.* **12** 046008
- [45] Morin A, Desreumaux N, Caussin J-B and Bartolo D 2017 Distortion and destruction of colloidal flocks in disordered environments *Nature Phys.* **13** 63